VLBA Imaging of NGC 4261: Symmetric Parsec-scale Jets and the Inner Accretion Region

Dayton L. Jones

Jet Propulsion Laboratory, California Institute of Technology

and

Ann E. Wehrle

Infrared Processing and Analysis Center, Jet Propulsion Laboratory,

California Institute of Technology

Received _____; accepted _____

ABSTRACT

We observed the nuclear region of NGC 4261 (3C270) with VLBI to determine the morphology of the central radio source on parsec scales, and in particular to see if the inner radio axis remained in the same direction as the kpc-scale jets or whether it was aligned with the apparent rotation axis of the nuclear disk imaged by HST. The position angle of the radio axis in our VLBA images agrees, within the errors, with the position angle of the VLA-scale jet. Thus, there is no evidence for precession of the jets on time scales shorter than the material propagation time from the nucleus to the diffuse radio lobes. Our dual frequency observations also reveal basically symmetric radio structures at both 1.6 and 8.4 GHz. Analysis of these images shows that most of the central 10 pc of this source is not significantly affected by free-free absorption, even though HST images of the the nucleus of the galaxy show it to contain a nearly edge-on disk of gas and dust on larger scales. The lack of detectable absorption over most of the central 10 pc implies that the density of ionized gas in this region is less than $\sim 10^3$ cm^{-3}, assuming a temperature of $\sim 10^4$K. Our highest angular resolution images show a very narrow absorption feature just east of the radio core, suggesting that there may be a small, dense inner accretion disk whose width is less than 0.1 pc. If the inclination of this inner disk is close to that of the larger-scale HST disk it becomes optically thin to 8.4 GHz radiation at a deprojected radius of about 0.8 pc. The brightness of the pc-scale jets falls off very rapidly on both sides of the core, suggesting that the jets are rapidly expanding during the first several pc of their travel. The rate of jet expansion must slow when the internal pressure falls below that of the external medium. We suggest that this occurs between about 10 and 200 pc from the core because the rate of decrease in radio brightness is far slower $>$ 200 pc from the core

than it is within 10 pc of the core. It appears that there is a small dense inner disk centered on the radio core (the base of the jets; < 1 pc), a low density, presumably hot "bubble" filling most of the the inner several pc of the nucleus (within which the radio jets expand rapidly; ~ 10 pc), and a surrounding cool, higher density region (of which the HST absorption absorption disk is part; > 10 pc) within which the transverse expansion of the radio jets, as implied by the rate of decrease in jet brightness, is nearly halted.

Subject headings: accretion, accretion disks — galaxies: active — galaxies: individual (NGC 4261, 3C270) — galaxies: jets — galaxies: nuclei

1. Introduction

The radio source 3C270 (PKS 1216+06) associated with the E2 galaxy NGC 4261 is composed of two symmetric lobes of extended emission on opposite sides of the galaxy, connected by symmetric kpc-scale jets to a compact radio source coincident with the optical nucleus of the galaxy. The compact radio core is a relatively weak VLBI source (180 mJy at 1.6 GHz; Jones, Sramek, and Terzian 1981). The radio jets extend out approximately ±4 arcmin, have opening angles of less than 5°, and are co-aligned to within 1° along position angle 88° (Birkinshaw and Davies 1985). The ratio of jet/counterjet surface brightness within a few arcseconds of the central compact source is only about 2:1, indicating that relativistic beaming effects are not strong on kpc scales. The minor axis position angle of the galaxy remains $69° \pm 2$ over a wide range of radii (van den Bosch, et al. 1994; Ferrarese, et al. 1996), 19° from the radio axis, but the stellar rotation axis is along position angle $153° \pm 4$ (Davies and Birkinshaw 1986) only 6° from the projected major axis of the galaxy. Evidently NGC 4261 is a nearly prolate galaxy whose stellar rotation axis has no relationship with the direction of the radio jets.

Möllenhoff and Bender (1987) discovered a small dust lane in the center of NGC 4261 which is oriented perpendicular to the radio jets. More recent HST observations have revealed that the optical nucleus is surrounded by a disk of gas and dust 1.7 arcsec in diameter whose projected rotation axis is aligned within several degrees of the radio jets (Jaffe, et al. 1993; 1996; Ferrarese, et al. 1996). At a distance of 41 Mpc (Faber et al. 1989) the HST disk diameter is 340 pc. Some authors give distance estimates up to three times smaller than this, which of course would reduce the calculated physical size of the HST disk by the same factor. The rotation axis of the HST disk is inclined 69° from our line of sight based on HST FOS spectral data, or 64° based on isophote fitting (Ferrarese, et al. 1996). These values agree within their errors. This suggests that the radio axis may

be at a similar angle from our line of sight.

The apparent inclination of the HST absorption disk and the larger-scale (Möllenhoff and Bender dust lane) disk differ by about 10°. It is likely that the HST disk and the larger scale dust lane are both part of a single warped disk structure (Mahabal et al. 1996). Since the minor axis of the HST disk is at a position angle of $63° \pm 2°$ (Ferrarese et al. 1996), which is not parallel to the position angle of the radio jets ($88° \pm 1°$; Birkinshaw and Davies 1985), the presumed warp continues into the region close to the central black hole. Jaffe et al. (1996) point out that the apparent center of the HST disk is displaced from the optical center of the galaxy (based on isophote fitting) by at least 5 pc (see also Ferrarese et al. 1996).

Neutral hydrogen and CO have been detected in absorption against the radio core by Jaffe and McNamara (1994). Their measurements indicate that the total mass of gas in the HST disk is $\sim 10^5$ $M_\odot$, which is sufficient to power the radio source for $\sim 10^8$ years. All of the above evidence suggests that the radio source is powered by material accreting in from the large-scale dust disk through the HST dust disk and eventually onto the (unseen) inner accretion disk where the radio jet formation takes place within a few Schwartzschild radii of a central massive black hole. The accreting material probably came from a merger between NGC 4261 and a smaller gas-rich galaxy. This would explain the apparently unrelated dynamics between the gas and dust in the nuclear disks and the over-all stellar dynamics of the galaxy.

We observed the nuclear region of NGC 4261 with VLBI to determine the morphology of the central radio source on parsec scales, and in particular to see if the inner radio axis remained in the same direction as the kpc-scale jets (position angle = 88°) or whether it was aligned with the apparent rotation axis of the HST disk.

2. Observations and Results

We observed NGC 4261 for 8.5 hours on 1 April 1995 using all ten antennas of the NRAO Very Long Baseline Array. Individual scans of typically 26 minutes duration were alternated between 1.6 GHz and 8.4 GHz. We recorded a bandwidth of 64 MHz with single polarization, and the data were cross-correlated on the VLBA correlator.

After cross-correlation the data were read into AIPS[1], where standard programs were used for editing, amplitude calibration, and fringe fitting. Prior to fringe fitting the strong compact radio source 1308+326 was used to derive corrections for phase slopes across the frequency channels at both 1.6 and 8.4 GHz. After fringe fitting the data were averaged over frequency and exported to the Caltech program Difmap (Shepherd, Pearson, and Taylor 1994) for additional editing, self-calibration, imaging, and deconvolution. Only marginal detections were obtained on the longest VLBA baselines (to the antennas at Saint Croix and Mauna Kea) at 1.6 GHz, but good fringes were found to all ten antennas at 8.4 GHz.

Our final VLBA images are shown in figures 1-5. Figures 1 and 2 are the highest dynamic range images at 1.6 and 8.4 GHz, respectively. At both frequencies the source appears two-sided, although the extension to the west (the direction of the slightly brighter VLA jet) falls off more slowly in brightness than the extension to the east. In neither image does the source appear to have a one-sided "core-jet" morphology. At a distance of 41 Mpc, 1 milliarcsecond (mas) corresponds to 0.20 pc. Consequently, the lengths of the visible radio jets (measured from the central brightness peak) are approximately 12 pc at 1.6 GHz and 4 pc at 8.4 GHz.

---

[1]The Astronomical Image Processing System was developed by the National Radio Astronomy Observatory, which is operated by Associated Universities, Inc., under a cooperative agreement with the National Science Foundation.

EDITOR: PLACE FIGURE 1 HERE.

EDITOR: PLACE FIGURE 2 HERE.

Figure 3 is our highest resolution image at 8.4 GHz made with full weighting of the longest baselines. Because the longest baselines have the lowest average signal-to-noise ratios, the noise level in figure 3 is nearly a factor of two greater than in figure 2. However, figure 3 does reveal a new feature which is not visible in lower resolution images: the very sharp eastern edge of the brightest peak. Our gray-scale image (figure 4) shows this to be a narrow gap in emission between the peak and the first obvious feature of the east-pointing jet. No such gap is seen on the western side of the source. Thus, the radio structure in figures 3 and 4 appears to be much less symmetric than that in figures 1 and 2. This is the expected signature of a small, dense inner accretion disk, whose apparent thickness is less than 0.5 mas or 0.1 pc. If real, this inner disk becomes optically thin at 8.4 GHz at a projected radius of about 1.5 mas (0.3 pc); the deprojected radius is smaller than 1 pc unless the inclination angle of the inner disk is larger than 72° (recall that the inclination angle of the much larger HST disk is $\approx 67°$).

EDITOR: PLACE FIGURE 3 HERE.

EDITOR: PLACE FIGURE 4 HERE.

If our interpretation of this gap as being the result of free-free absorption by an inner accration disk is correct, it is perhaps surprising that an even larger absorption feature is not seen in our 1.6 GHz images. To investigate this, we simulated the one-dimensional

brightness distribution of an intrinsically symmetric source with a narrow gap on one side and convolved this profile with Gaussian beams of different widths. We found that it is possible for the simulated absorption feature to be easily visible with the VLBA 8.4-GHz beam but invisible with the 1.6 GHz beam, which is more than five times as wide. In fact, the actual beam used at 1.6 GHz is nearly ten times as wide as the full-resolution 8.4 GHz beam because we downweighted the low SNR data on the longest baselines at 1.6 GHz to improve the dynamic range.

Figure 5 is an image at 8.4 GHz which was made by applying a Gaussian taper to the visibility data to match the angular resolution available at 1.6 GHz. The same field of view and restoring beam has been used for figures 1 and 5 to allow easy comparison.

EDITOR: PLACE FIGURE 5 HERE.

Although the degree of symmetry depends on both frequency and angular resolution, the source appears basically two-sided in all of the above figures. The more symmetric appearance at 1.6 GHz is partially caused by the greater extent of the jets at 1.6 GHz due to spectral index effects, and also suggests that the cause of the "gap" in figures 3 and 4 is confined to an angular scale much smaller than the 1.6 GHz or tapered 8.4 GHz beams.

Attempts were made to detect more distant emission at both 1.6 and 8.4 GHz using larger image sizes and tapering the visibility data to favor short baselines. In no case did we find any emission significantly more extended than that shown in figures 1 and 5, although the range of VLBA baselines would allow more extended radio structure to be detected. We conclude that the brightness of the two parsec-scale radio jets does drop below our noise level very rapidly at both frequencies, and that this is not an artifact of the imaging procedure.

In referring to the images in figures 1-5 as symmetric or two-sided, we are implicitly

assuming that the central brightness peak is the "core" of the source (the base of the radio jets). Is there any evidence to support this assumption? We have compared the images in figures 1 and 5 to determine spectral index distributions for a range of position offsets between the two images. Figure 6 shows the spectral index distribution along the east-west axis of the source when the central peaks at both frequencies are aligned. Not surprisingly, the spectral index distribution is also quite symmetric with an inverted spectrum near the center and increasingly steep spectra with increasing distance from the center. It is possible to offset the 8.4 GHz peak up to 10-12 mas from the 1.6 GHz peak without making the spectral index $\alpha > +2.5$ (using $S_\nu \propto \nu^\alpha$), but in this case the spectral index more than ≈ 30 mas from the center becomes extremely steep ($\alpha < -2$). We therefore favor a registration in which the brightest peaks in figures 1 and 5 are nearly co-aligned, giving a spectral index distribution close to that shown in figure 6.

EDITOR: PLACE FIGURE 6 HERE.

The inverted spectrum at the center of the source could be caused by synchrotron self-absorption or by free-free absorption. In the case of free-free absorption the ionized gas responsible for the inverted spectrum at the center of the source would have to cover only the inner 0.2-0.3 pc and/or have a filling factor substantially less than unity to account for the fact that $\alpha < 1$. Free-free absorption by thermal gas uniformly covering a source gives an inverted spectrum with $\alpha \approx 2$. Synchrotron self-absorption is seen in the cores of many compact extragalactic radio sources, and by analogy we might expect to see this effect in the core of NGC 4261. Our brightness temperatures (see below) are lower limits, and therefore they do not rule out synchrotron self-absorption, which can produce inverted spectra with $\alpha \leq 2.5$ depending on the turn-over frequency and homogeneity of the source. We can not exclude a combination of both effects in the center of NGC 4261. In both morphology and spectral index distribution NGC 4261 is very similar to the parsec-scale

source in Hydra A (Taylor 1996).

The brightness of both the east and west jets drops off rapidly at both frequencies. To quantify this, we found that three of the four brightness profiles could be reasonably well fit with a power law of the form (surface brightness) $\propto$ (distance from peak)^x. At 1.6 GHz the exponent x is -1.9 for the jet extending to the west and -2.0 for the jet extending to the east. The linear brightness profile fits for 1.6 GHz are shown in figure 7.

EDITOR: PLACE FIGURE 7 HERE.

Although the western jet fades slightly more slowly with distance from the core, these values are very similar. At 8.4 GHz the corresponding exponents are x = -1.2 for the western jet and -2.0 for the eastern jet. Again, the eastern jet fades more rapidly. The eastern jet at 8.4 GHz is not very well fit by a single exponential law, although the western jet is. The 8.4 GHz brightness profile fits are shown in figure 8.

EDITOR: PLACE FIGURE 8 HERE.

In all cases we used measurements of the brightness per unit length (Jy/mas) starting near 50% of the peak value and extending out in steps of 0.7-0.8 times the half power beamwidth (6.5 mas steps at 1.6 GHz and 1.2 mas steps at 8.4 GHz). This represents a compromise between having truly independent measurements and having an adequate number of points for the least-squares fit.

The total flux density of the VLBI structure shown in figures 1 and 3 is 0.20 Jy at 1.6 GHz and 0.34 Jy at 8.4 GHz. The peak (core) surface brightness is 0.10 Jy/beam at both 1.6 GHz and 8.4 GHz. This corresponds to a brightness temperature of 3.3×10^8K at 1.6 GHz and 1.2×10^9K at 8.4 GHz; these values are lower limits to the true brightness temperature of the core, which is angularly unresolved at both frequencies.

The VLBI position angles are $86.2° \pm 1.5°$ at 1.6 GHz and $85.6° \pm 1.5°$ at 8.4 GHz. At both frequencies the VLBI position angles are consistent (within the combined errors) with the $88° \pm 1°$ position angle of the VLA jets, although the 8.4 GHz value may suggest a small curvature of the jets very close to the core. If real, this curvature makes the inner jet orientation slightly closer to the minor axis of the HST disk ($73° \pm 2°$; Ferrarese et al. 1996). Higher frequency VLBI observations will be needed to determine the reality of any jet curvature in the central few pc of this source.

3. Discussion

It is clear from VLA images that both the east and west jet in NGC 4261 extend far beyond the scale of our VLBA images. Therefore, the disappearance of both jets within a few tens of mas of the core is not caused by their disruption or "smothering" by a dense interstellar medium. It is possible that the jets are fading due to expansion close to the core. This implies that the external pressure is less than the internal jet pressure. At some point the internal pressure in the expanding jets will become lower than the external pressure (which should fall more slowly than d^{-2} at large distances), causing the opening angle of the jets to be reduced and possibly creating shocks which could reaccelerate the relativistic electrons. The result will be a much slower decrease in jet brightness on kpc scales. Our angular resolution is insufficient to measure the opening angle of the pc-scale jets, but from figure 2 we can get an upper limit of approximately 10° for the east jet, compared with less than 5° on kpc scales.

We can set an upper limit on the free electron density in the inner ~ 10 pc of NGC 4261 from the apparent lack of free-free absorption of either jet at 1.6 GHz. If absorption by a 10-pc-scale disk or torus of ionized gas were significant, we would expect to see a much more asymmetric radio morphology in figures 1 and 2 (*cf.* 3C84; Vermeulen, Readhead,

and Backer 1994; Walker, Romney, and Benson 1994). Since both east and west jets in NGC 4261 are visible out to $\sim$ 10 pc with similar brightness, the optical depth from free-free absorption must be much less than unity. Assuming a gas temperature of $\sim 10^4$K and a path length of 10 pc gives an electron density $< 10^3$ cm^{-3}. Note however that our limit applies to the inner few pc of NGC 4261 as a whole; the apparent absorption on a sub-pc scale in figures 3 and 4 would be undetectable at lower angular resolutions. Thus, we are not ruling out free-free absorption by a high electron density gas within the central pc. If the path length through the inner disk suggested by figures 3 and 4 is assumed to be ~ 0.1 pc, the resulting lower limit for n_e is $\sim 10^5$ cm^{-3}.

For NGC 4261 the total mass of ionized gas implied in the inner 10 pc, neglecting the possible sub-pc inner disk, is $< 10^5$ M$_\odot$. It appears that we have a low density, presumably hot, inner "bubble" filling the inner several pc of the nucleus (within which the radio jets expand rapidly) surrounded by a cool, higher density region (of which the HST absorption disk is part) within which the transverse expansion of the radio jets is nearly halted. Higher electron densities have been estimated from optical observations (Jaffe, et al. 1996; Ferrarese, et al. 1996), but the angular resolution of these measurements is no better than 0.1 arcsec and consequently they may be partially sampling a higher density region surrounding the region in which we see the VLBI radio jets. Another possibility is that much of the optical emission comes from within the central pc, in which case a small region of higher density gas could dominate the optical measurements.

As Bridle and Perley (1984) point out, the central brightness of an expanding synchrotron jet decreases as a different power of distance (or radius) d depending on whether the jet is dominated by a parallel or transverse magnetic field, or if equipartition is assumed. Our VLBI images do not resolve the jets in the transverse direction, so we measure the brightness per unit length rather than the surface brightness. For an optically

thin jet with $\alpha = -0.65$ the brightness per unit length falls off as $d^{-4.2}$ for a parallel magnetic field, $d^{-2.5}$ for a transverse magnetic field, and $d^{-3.1}$ if equipartition is assumed. All of these exponents are more negative than the observed fall-off of brightness per unit length in the parsec-scale jets of NGC 4261. This is a common result for many radio jets (e.g., Perley, Bridle, and Willis 1984), and it implies than magnetic field amplification and/or particle reacceleration (or a dramatic reduction in jet velocity) must take place as the jet expands. Based on figure 5, the jets in NGC 4261 appear to be optically thin only at distances greater than 10-15 mas from the core. This complicates the interpretation of the brightness profiles at 8.4 GHz, but at 1.6 GHz the jet profiles with their d^{-2} fall-off extend well beyond this region.

Taylor (1996) presents VLBA images and spectral index maps of the central radio source in Hydra A which look remarkably similar to those presented in this paper. Taylor finds evidence for significant ($\tau > 1$) free-free absorption of the radio core in Hydra A at 1.3 GHz and deduces a value of $r\ {n_e}^2$ which is equal to the upper limit we find for NGC 4261. At our lowest frequency of 1.6 GHz the free-free absorption deduced by Taylor would have an optical depth < 1. If the thermal gas density in the nucleus of NGC 4261 is somewhat smaller than in Hydra A, the effects of free-free absorption would be quite small at our observing frequencies. The neutral hydrogen column density in front of the radio core in NGC 4261 is approximately 20 times smaller than in Hydra A (Jaffe and McNamara 1994; Taylor 1996).

Another method for estimating hydrogen column density is through X-ray absorption. NGC 4261 contains an X-ray source whose angular extent is similar to that of the optical galaxy (Fabbiano, Kim, and Trinchieri 1992; Worrall and Birkinshaw 1996), as well as fainter emission on larger scales (Worrall and Birkinshaw 1994; Davis, et al. 1995) and a strong component which is angularly unresolved by ROSAT (Worrall and Birkinshaw 1994;

1996). Birkinshaw and Worrall (1996) concluded that the extended X-ray gas confines the kpc-scale radio jets, and that the jets terminate (flair into the two diffuse lobes) at the point where the external pressure falls below the internal pressure in the jets. This implies that the flow in the jets is subsonic. Einstein IPC spectra can be fit with a power law (Kim, Fabbiano, and Trinchieri 1992), but a thermal plus power law spectrum provides the best fit to ROSAT data (Worrall and Birkinshaw 1994). In the thermal plus power law model the derived neutral hydrogen column density in NGC 4261 is quite small ($N_H < 4 \times 10^{20}$ atoms cm^{-2}), and the cooling time for gas within the core radius is estimated to be 3.4×10^9 years. The low hydrogen column density derived from the X-ray data are difficult to reconcile with the higher HI densities derived from the radio absorption measurements of Jaffe and McNamara (1994). Worrall and Birkinshaw (1994) discuss several possible reasons for this difference. One explanation is that the radio emission comes to us directly from the core and inner regions of the jets, and consequently at least partly through the suggested dense inner accretion disk, while the X-ray emission (the nonthermal power law component) is initially directly in the same general direction as the radio jets and is scattered into our line of sight by plasma within the jet or surrounding the inner nuclear region. If this proposed X-ray scattering occurs far enough from the radio core, the gas density along the mean X-ray line of sight could be substantially smaller than along the mean radio line of sight. This model predicts that future very high angular resolution X-ray images of the NGC 4261 nucleus will find a position offset between the radio and X-ray peaks, and that this offset will be approximately along the direction of the radio jets. An alternative possibility is that the X-ray emission comes from an angularly larger region than the bright central radio source; this would have the same effect of allowing most of the X-ray emission to avoid the presumed inner accretion disk.

The position angle of the radio axis in our VLBA images agrees, within the combined errors, with the position angle of the VLA-scale jets. Thus there is no evidence for

precession of the jets on time scales shorter than the material propagation time from the nucleus to the diffuse radio lobes. This long-term stability implies that the central compact object has a very large angular momentum.

If the central black hole in NGC 4261 is $10^8 - 10^9$ $M_\odot$ it is unlikely that it would have any detectable orbital motion about a presumably less massive secondary nucleus from a merger (which could be the cause of the positional offset between the apparent center of the HST dust disk and the radio core). In this case the secondary nucleus (and perhaps parts of the nuclear gas disk) would show almost all of the orbital motion. This could also explain the small but significant difference between the radio jet position angle and the position angle of the HST disk rotation axis.

4. Conclusions

We have found that the pc-scale radio source in the nucleus of NGC 4261 is unusually symmetric, and aligned along the same position angle as the larger-scale radio structure imaged with the VLA. The morphology and spectral index distribution of the pc-scale source indicates that free-free absorption is not significant within several pc of the radio core, except possibly within the central pc. The brightness of both radio jets decreases very rapidly in both directions from the core, which we interpret as evidence for a large initial opening angle (rapid expansion). At some distance between about 50 and 500 pc the jet opening angles decrease to the $< 5^\circ$ value seen on kpc scales. This should occur when the internal jet pressure falls below that of the external medium.

We thank David Meier for several informative discussions about jet collimation, D. Worrall for information on the large scale X-ray morphology, and the anonymous referee for several corrections and suggestions which significantly improved this paper. The Very

Long Baseline Array is part of the National Radio Astronomy Observatory, which is a facility of the National Science Foundation operated by Associated Universities, Inc., under a cooperative agreement with the NSF. A.W. gratefully acknowledges support from the NASA Long Term Space Astrophysics Program. This research was carried out at the Jet Propulsion Laboratory, California Institute of Technology, under contract with the National Aeronautics and Space Administration.

REFERENCES

Bridle, A. H., and Perley, R. A. 1984, ARA&A, 22, 319

Birkinshaw, M., and Davies, R. L. 1985, ApJ, 291, 32

Birkinshaw, M., and Worrall, D. M. 1996, Energy Transport in Radio Galaxies and Quasars, eds. P. E. Hardee, A. H. Bridle, and A. Zensus (ASP Conf. Series, vol. 100), 335

Davies, R. L., and Birkinshaw, M. 1986, ApJ, 303, L45

Davis, D. S., Mushotzky, R. F., Mulchaey, J. S., Worrall, D. M., Birkinshaw, M., and Burstein, D. 1995, ApJ, 444, 582

Fabbiano, G., Kim, D.-W., and Trinchieri, G. 1992, ApJS, 80, 531

Faber, S. M., Wegner, G., Burstein, D., Davies, R. L., Dressler, A., Lynden-Bell, D., and Terlevich, R. J. 1989, ApJS, 69, 763

Ferrarese, L., Ford, H. C., and Jaffe, W. 1996, ApJ, 470, 444

Ford, H., Ferrarese, L., and Jaffe, W. 1995, BAAS, 27, 1367

Jaffe, W., Ford, H. C., Ferrarese, L., van den Bosch, F., and O'Connell, R. W. 1993, Nature, 364, 213

Jaffe, W., and McNamara, B. R. 1994, ApJ, 434, 110

Jaffe, W., Ford, H., Ferrarese, L., van den Bosch, F., and O'Connell, R. W. 1996, ApJ, 460, 214

Jones, D. L., Sramek, R. A., and Terzian, Y. 1981, ApJ, 246, 28

Kim, D.-W., Fabbiano, G., and Trinchieri, G. 1992, ApJS, 80, 645

Mahabal, A., Kembhavi, A., Singh, K. P., Bhat, P. N., and Prabhu, T. P. 1996, ApJ, 457, 598

Möllenhoff, C., and Bender, R. 1987, A&A, 174, 63

Perley, R. A., Bridle, A. H., and Willis, A. G. 1984, ApJS, 54, 291

Shepherd, M. C., Pearson, T. J., and Taylor, G. B. 1994, BAAS, 26, 987

Taylor, G. B. 1996, ApJ, 470, 394

van den Bosch, F. C., Ferrarese, L., Jaffe, W., Ford, H. C., and O'Connell, R. W. 1994, AJ, 108, 1579

Vermeulen, R. C., Readhead, A. C. S., and Backer, D. C. 1994, ApJ, 430, L41

Walker, R. C., Romney, J. D., and Benson, J. M. 1994, ApJ, 430, L45

Worrall, D. M., and Birkinshaw, M. 1994, ApJ, 427, 134

Worrall, D. M., and Birkinshaw, M. 1996, Röntgenstrahlung from the Universe, eds. H. U. Zimmermann, J. Trümper, and H. Yorke (MPE Report 263), 531

Fig. 1.— VLBA image of NGC 4261 at 1.632 GHz. The contour levels are -0.5, -0.25, 0.25, 0.5, 1, 2, 4, 8, 16, 32, 50, 70, and 95% of the peak surface brightness (98 mJy/beam). The restoring beam is 14.70×9.11 mas with the major axis along position angle -10.5°.

Fig. 2.— VLBA image of NGC 4261 at 8.387 GHz. The contour levels are -0.25, 0.25, 0.5, 1, 2, 5, 8, 16, 32, 50, 70, and 95% of the peak surface brightness (149 mJy/beam). The restoring beam is 2.69×1.56 mas with the major axis along position angle -2.2°.

Fig. 3.— Full resolution VLBA image of NGC 4261 at 8.387 GHz. The contour levels are -0.5, 0.5, 1, 2, 4, 8, 16, 32, 70, 70, and 95% of the peak surface brightness (101 mJy/beam). The restoring beam is 1.84×0.80 mas with the major axis along position angle -1.1°.

Fig. 4.— Gray scale representation of the full-resolution 8.387 GHz image, showing the narrow gap in emission just east of the brightest peak (core).

Fig. 5.— Low resolution VLBA image of NGC 4261 at 8.387 GHz. The contour levels are -0.12, -0.06, 0.06, 0.12, 0.25, 0.5, 1, 2, 4, 8, 16, 32, 50, 70, and 95% of the peak surface brightness (288 mJy/beam). For comparison with figure 1 the same field of view and restoring beam (14.70×9.11 mas, position angle = -10.5°) has been used.

Fig. 6.— The spectral index α between 1.6 GHz and 8.4 GHz as a function of distance along the radio axis (PA = 88°). These values were determined by aligning the brightest peak at both frequencies (see figures 1 and 4). The small peak about 32 mas east (right) of the core is caused by the knot of emission visible in the eastern jet at 8.4 GHz (see figures 2 and 3).

Fig. 7.— Profile of brightness per unit length at 1.6 GHz along position angle 87°. **a)** East-pointing jet, **b)** West-pointing jet. The slope of the least-squares fit line is -2.0 for the east jet and -1.9 for the west jet. The distance between measurements is 6.5 mas except for the innermost point of the east jet. The projected restoring beam is a Gaussian with 9.23 mas full width at half maximum.

Fig. 8.— Profile of brightness per unit length at 8.4 GHz along position angle 87°. **a)** East-pointing jet, **b)** West-pointing jet. The slope of the least-squares fit line is -2.0 for the east jet and -1.2 for the west jet. Note that at this frequency the east jet is not well fit by a single power law. The distance between measurements is 1.2 mas and the projected restoring beam is a Gaussian with 1.56 mas full width at half maximum.

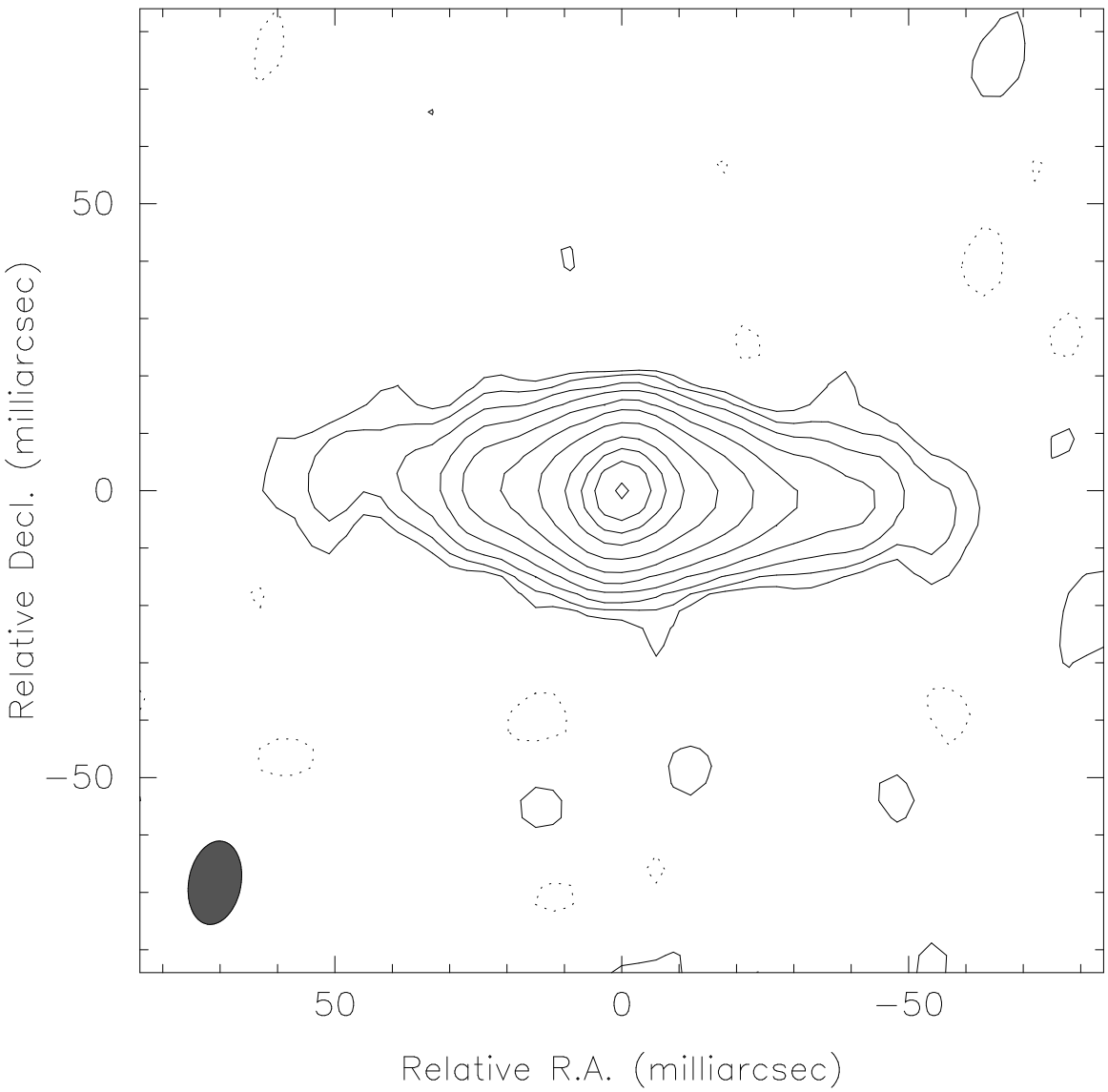
50
0
−50
Relative Decl. (milliarcsec)
50
0
−50
Relative R.A. (milliarcsec)

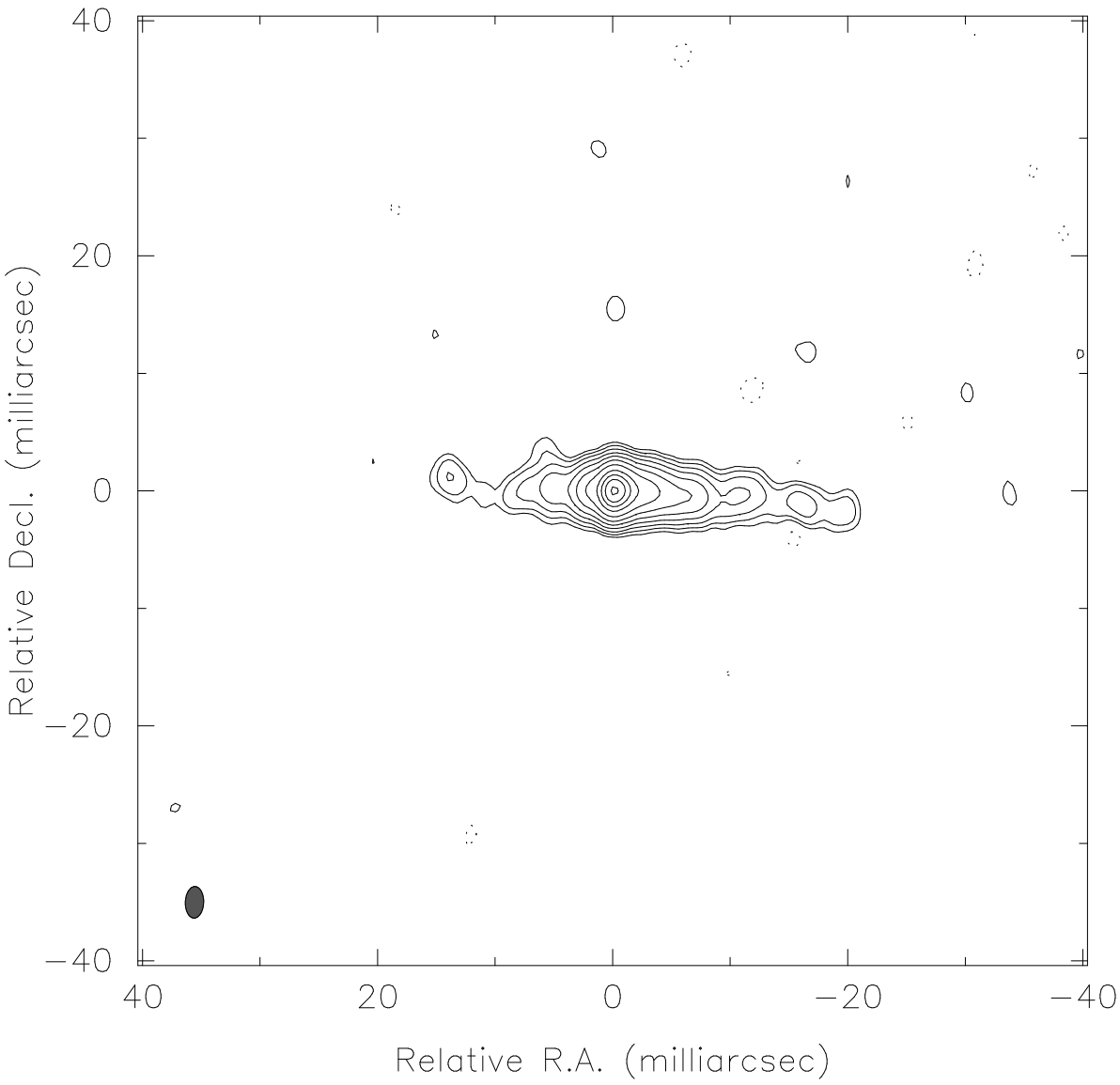
40
20
0
−20
−40
Relative Decl. (milliarcsec)
40
20
0
−20
−40
Relative R.A. (milliarcsec)

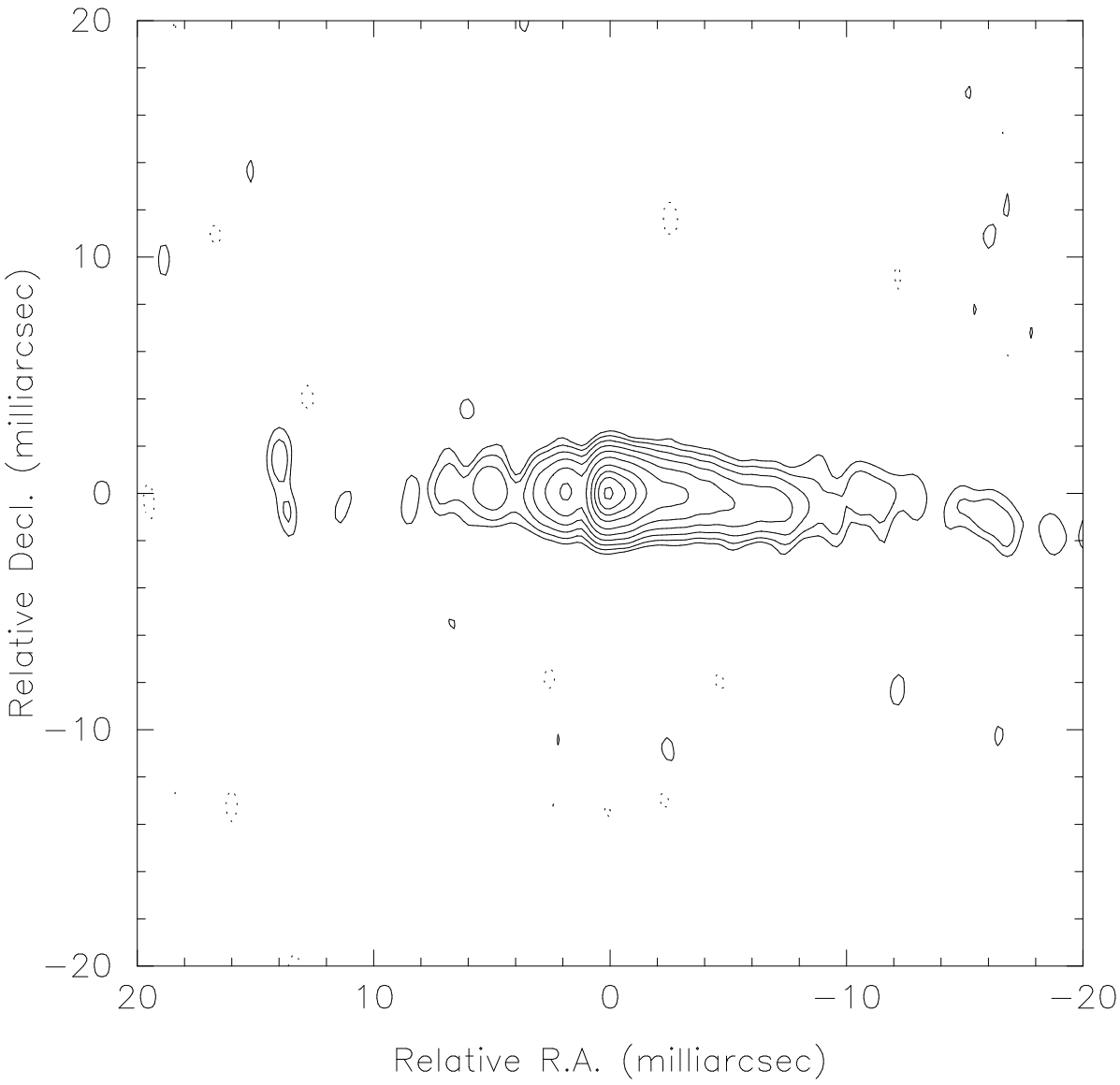
20
10
0
−10
−20
Relative Decl. (milliarcsec)
20
10
0
−10
−20
Relative R.A. (milliarcsec)

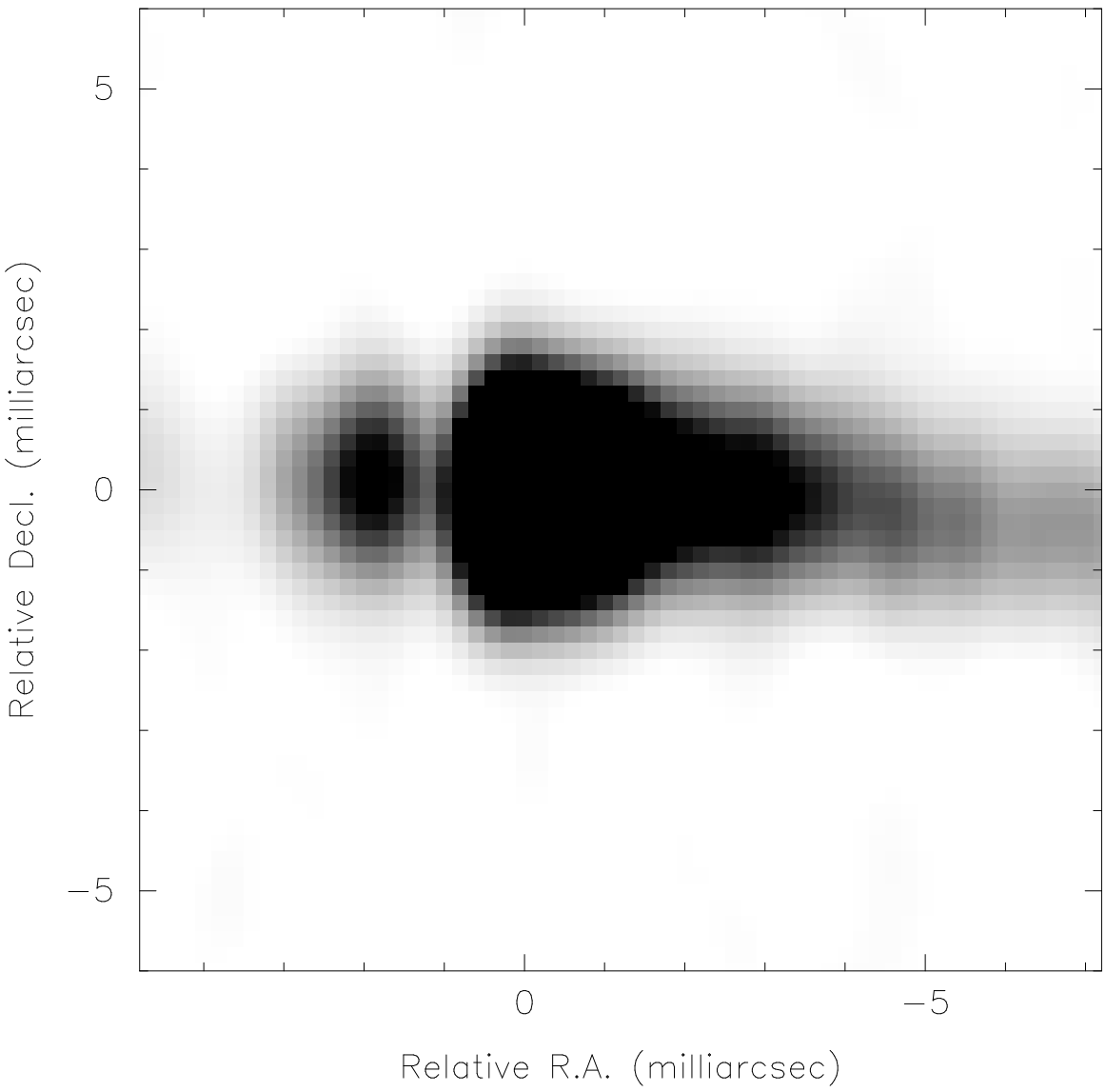
5
0
−5
Relative Decl. (milliarcsec)
0
−5
Relative R.A. (milliarcsec)

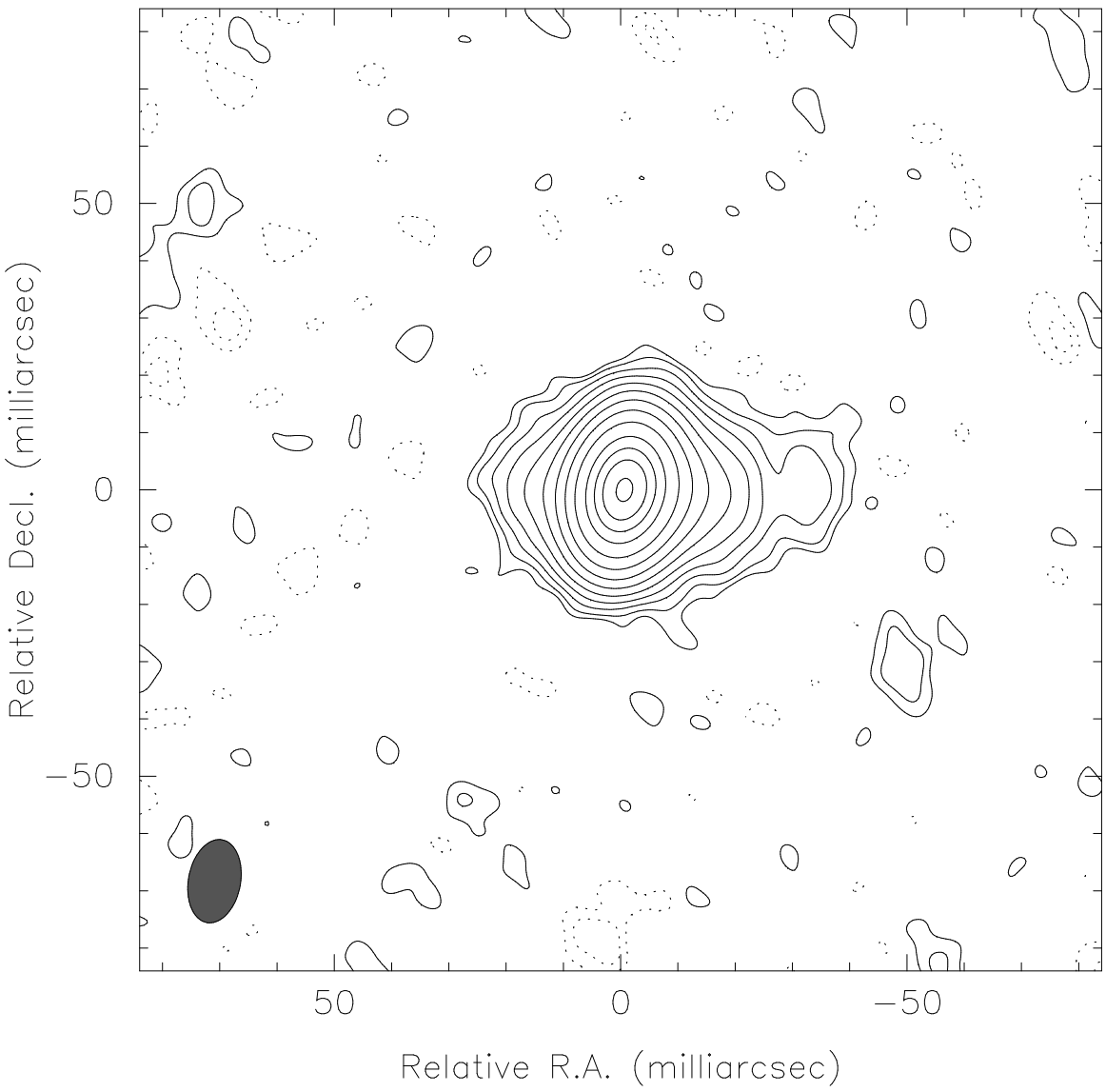
50
0
−50
Relative Decl. (milliarcsec)
50
0
−50
Relative R.A. (milliarcsec)

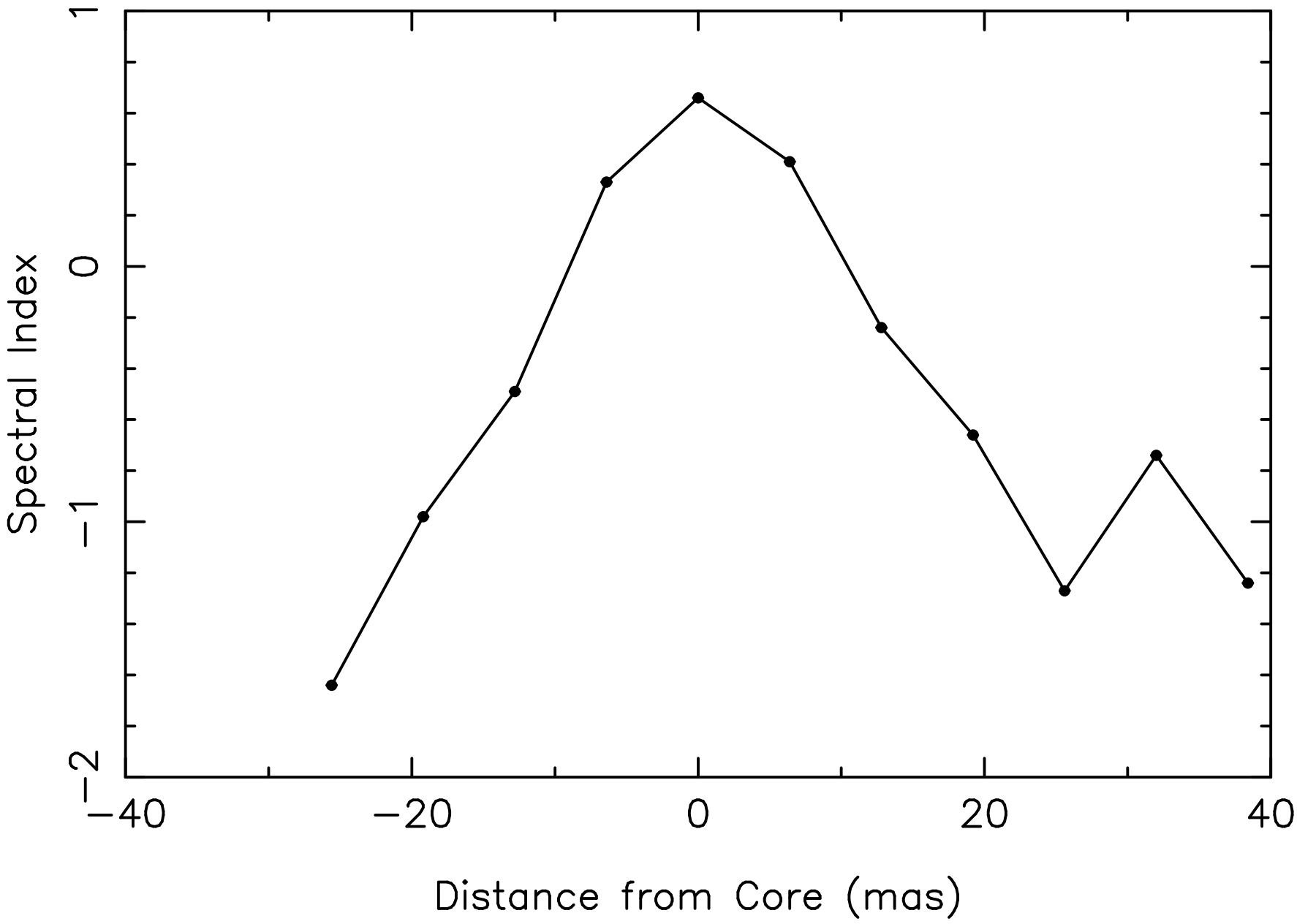
Spectral Index
1
0
−1
−2
−40
−20
0
20
40
Distance from Core (mas)

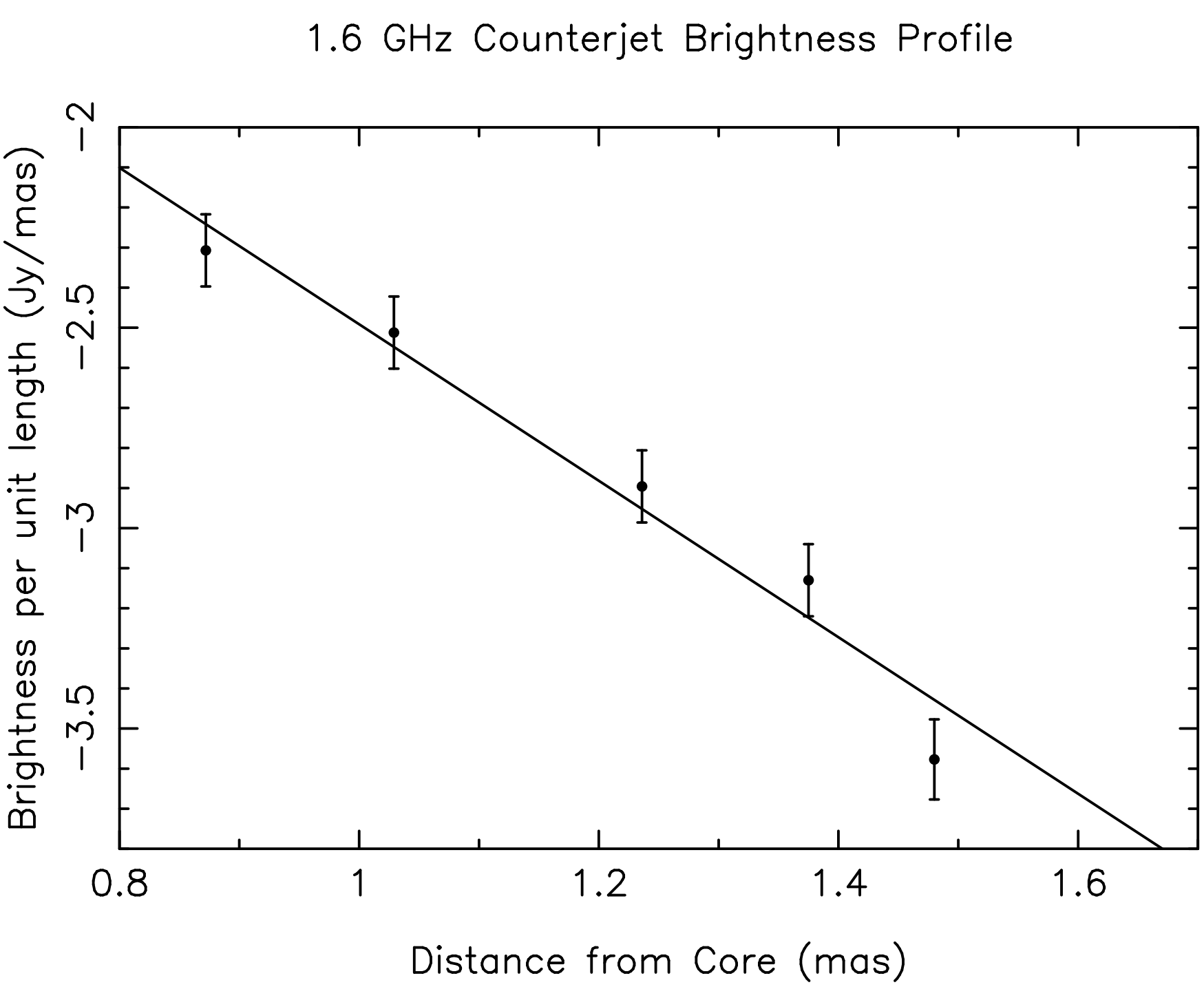
1.6 GHz Counterjet Brightness Profile
Brightness per unit length (Jy/mas)
−2
−2.5
−3
−3.5
0.8
1
1.2
1.4
1.6
Distance from Core (mas)

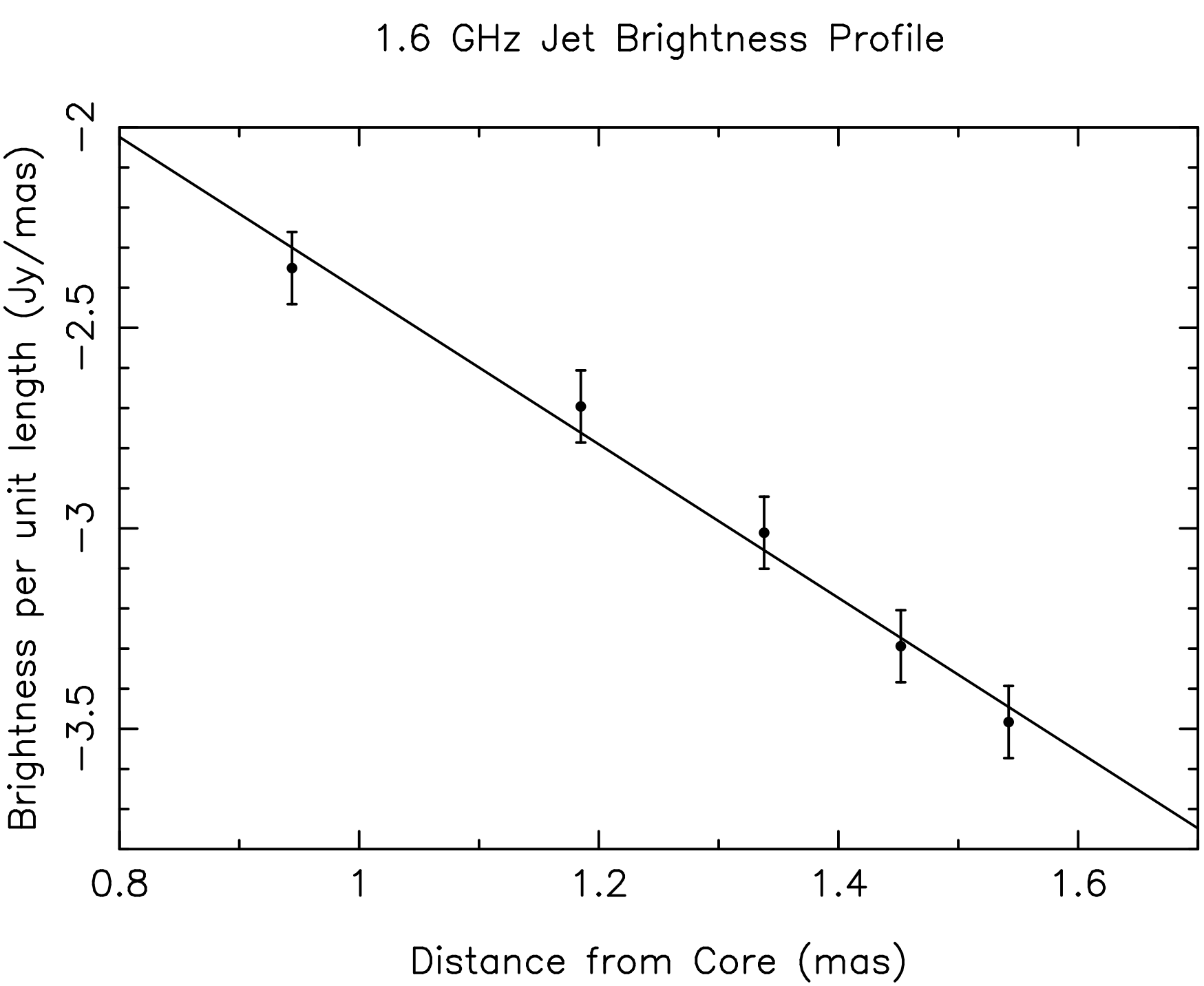
1.6 GHz Jet Brightness Profile
Brightness per unit length (Jy/mas)
−2
−2.5
−3
−3.5
0.8
1
1.2
1.4
1.6
Distance from Core (mas)

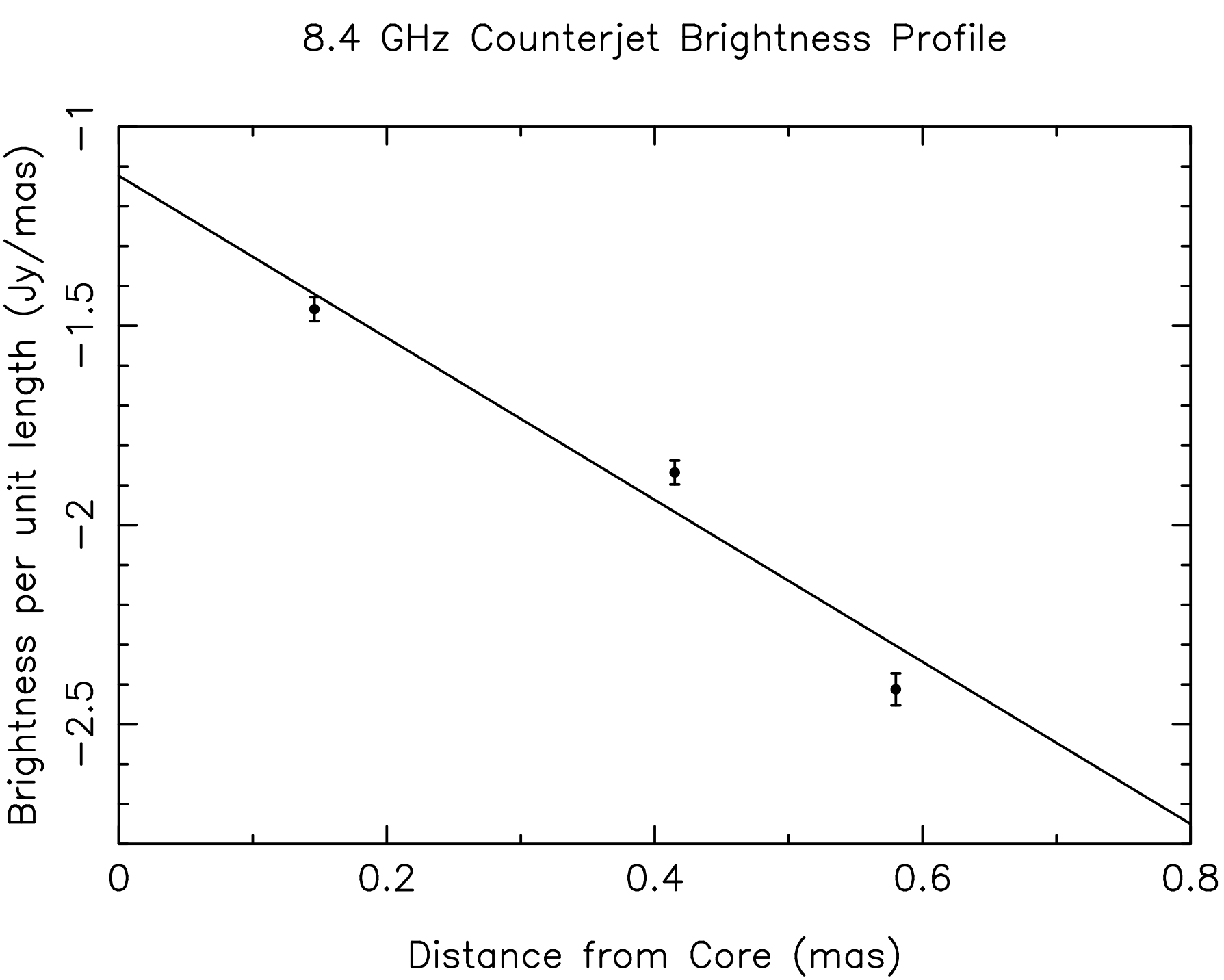
8.4 GHz Counterjet Brightness Profile
Brightness per unit length (Jy/mas)
−1
−1.5
−2
−2.5
0
0.2
0.4
0.6
0.8
Distance from Core (mas)

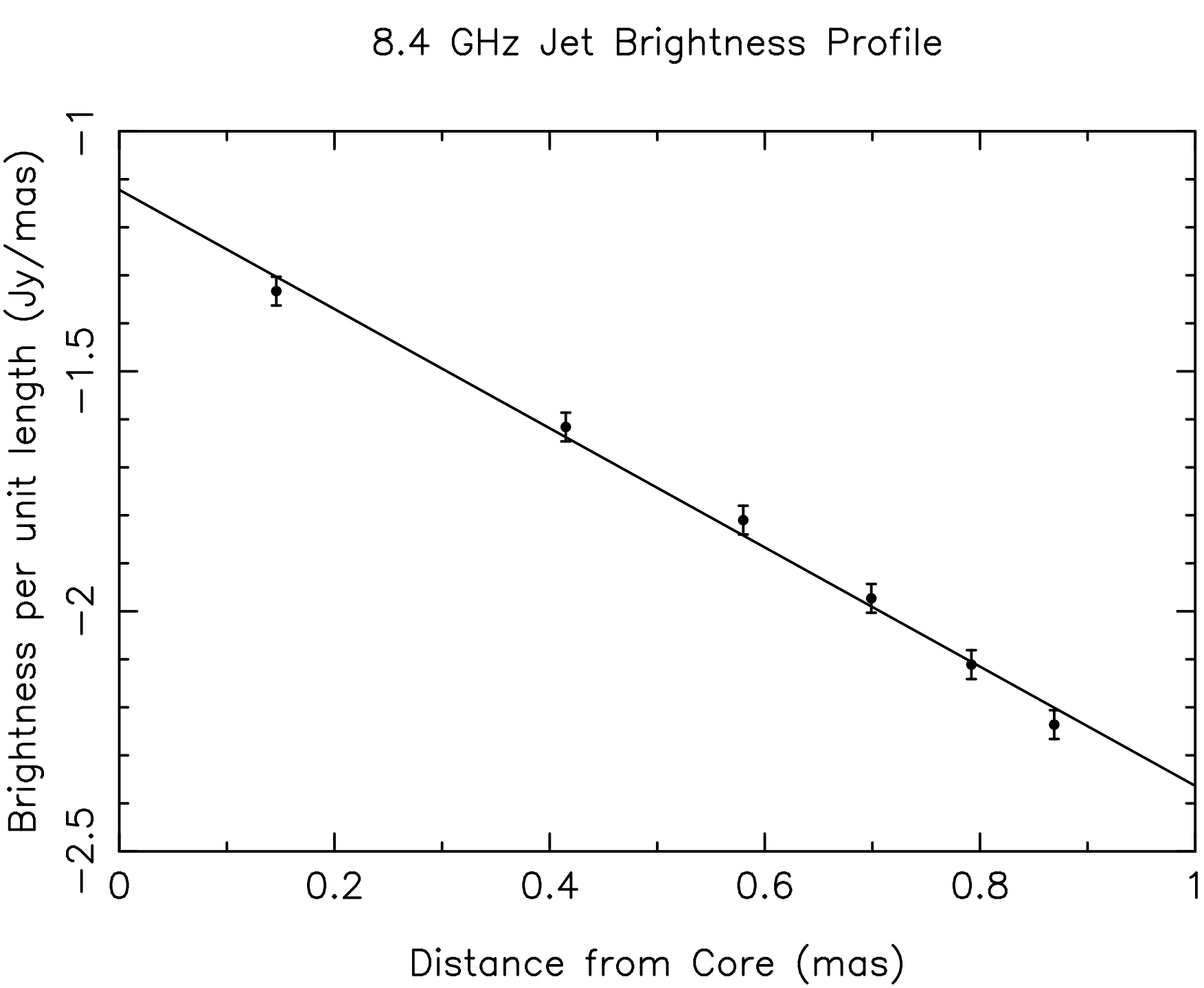
8.4 GHz Jet Brightness Profile
Brightness per unit length (Jy/mas)
−1
−1.5
−2
−2.5
0
0.2
0.4
0.6
0.8
1
Distance from Core (mas)